Paper presentation - 5

NANO LETTERS

Letter

Cite This: Nano Lett. 2018, 18, 1130−1138

pubs.acs.org/NanoLett

In Situ Investigation on the Nanoscale Capture and Evolution of Aerosols on Nanofibers

Rufan Zhang,[†] Bofei Liu,[†] Ankun Yang,[†] Yangying Zhu,[†] Chong Liu,[†] Guangmin Zhou,[†] Jie Sun,[†] Po-Chun Hsu,[†] Wenting Zhao,[†] Dingchang Lin,[†] Yayuan Liu,[†] Allen Pei,[†] Jin Xie,[†] Wei Chen,[†] Jinwei Xu,[†] Yang Jin,[†] Tong Wu,[†] Xuanyi Huang,[†] and Yi Cui[*,†,‡]

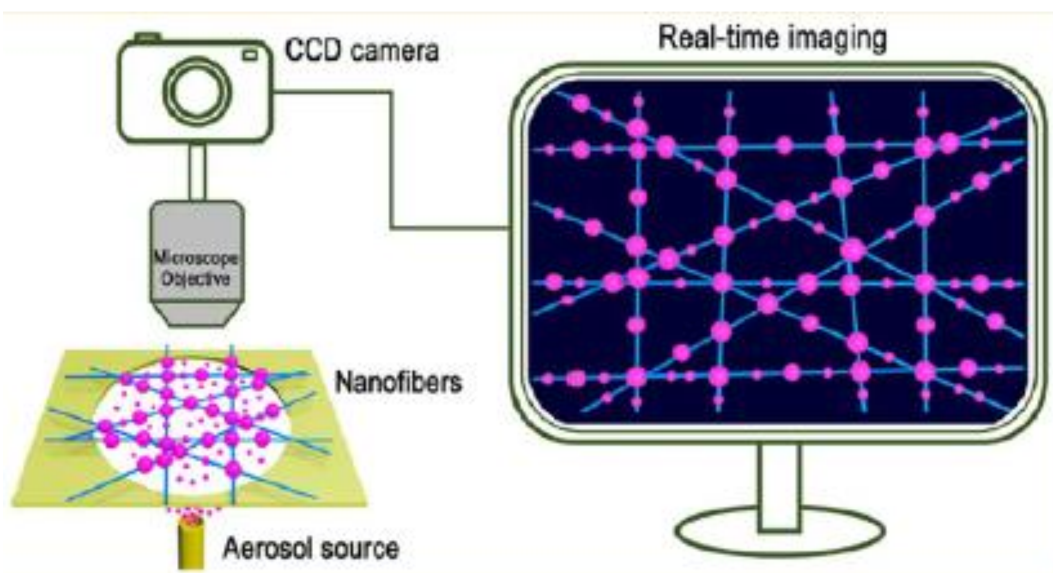

- P. Srikrishnarka

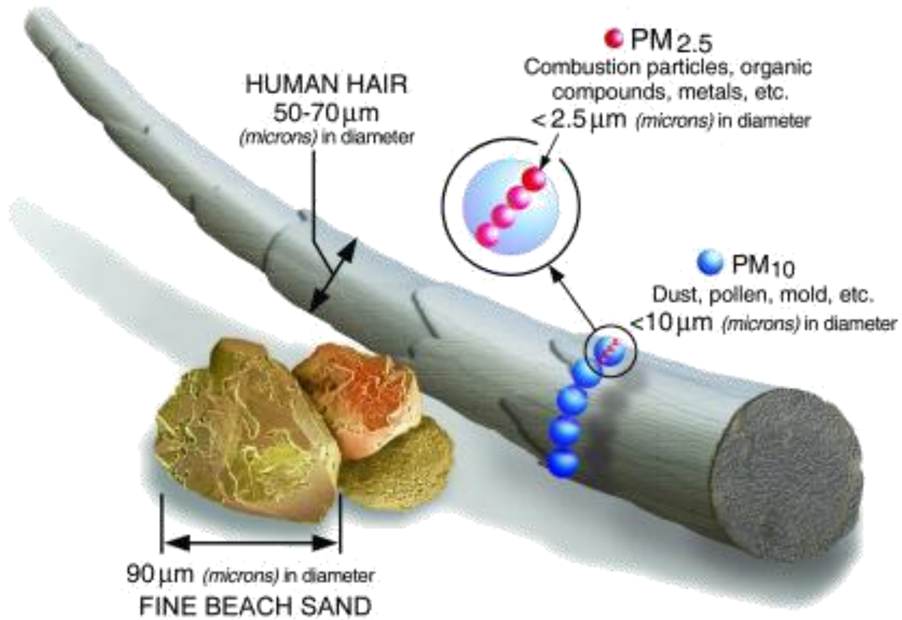

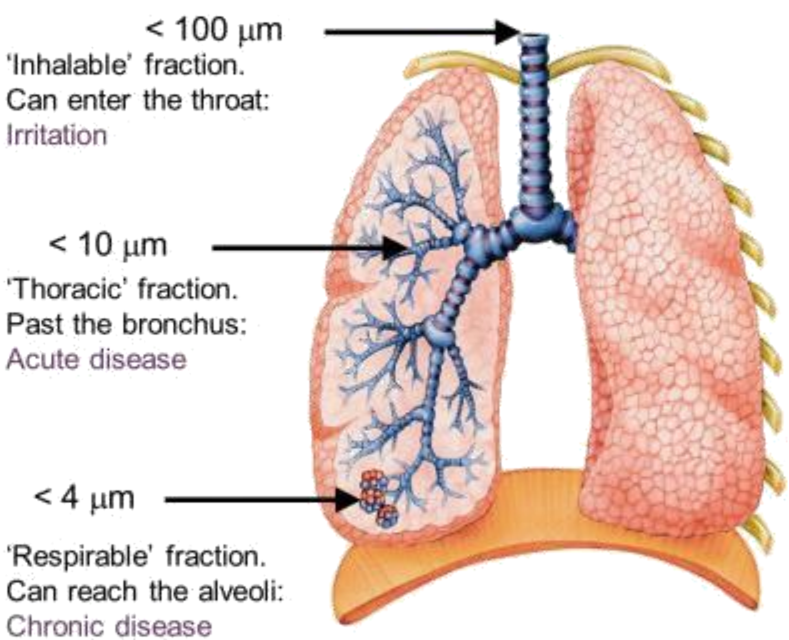

*https://www.epa.gov/pm-pollution/particulate-matter-pm-basics
**https://volcanoes.usgs.gov/volcanic_ash/respiratory_effects.html
***https://en.wikipedia.org/wiki/HEPA

$PM_{2.5}$ can penetrate human bronchi and even alveolar cells and can cause serious threat to health.

Filtration is one technique used to remove these PM.

Filtration is classically done by:
- Brownian diffusion,
- inertial impact
- Gravity Settling
- Electrostatic deposition

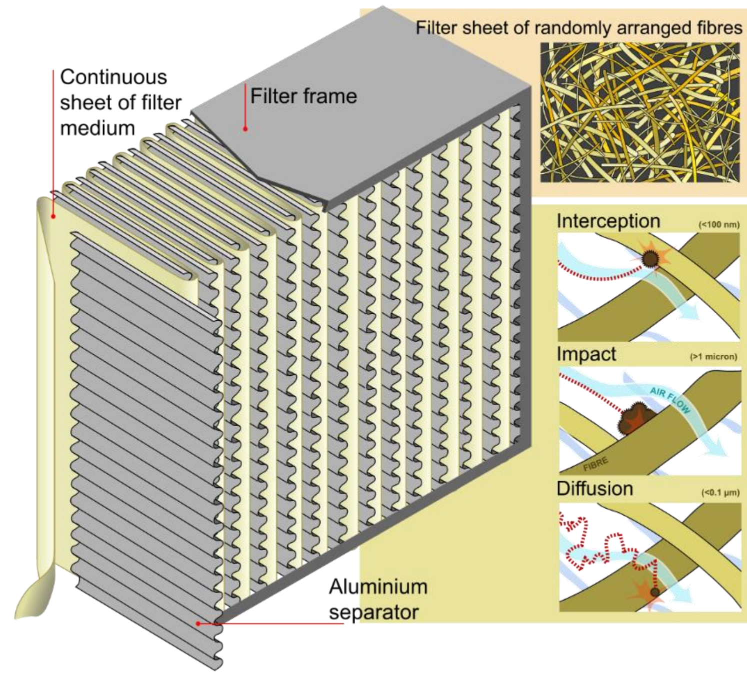

- ❑ In-situ wettability aspect of aerosols generated during electrospray could dictate the morphology of the particles
- ❑ In-situ nucleation of water droplets during AWC on surface will provide information for its increase or decrease of volume

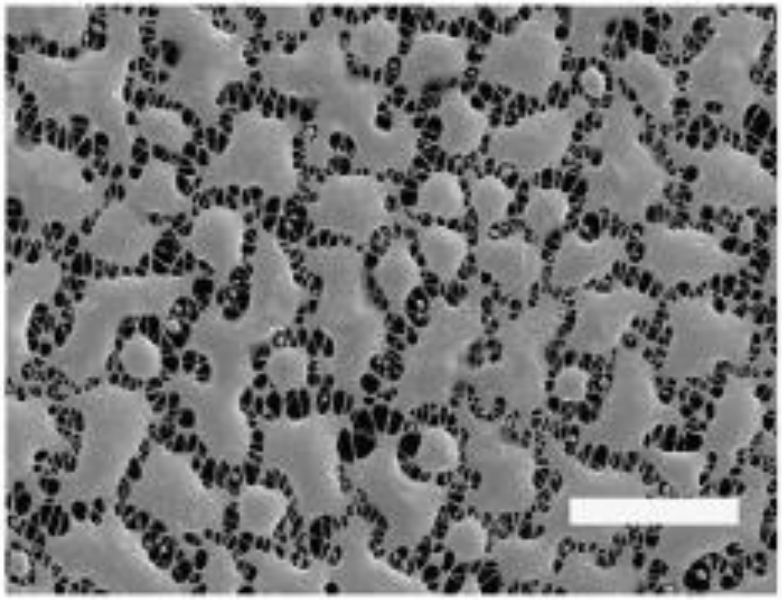

SEM showing the PAN transparent air filter morphology after 100-h PM capture test. Scale bars 50 μm

Filtration studies were mainly based on ex-situ and bulk analysis

This will not preserve the in situ and dynamic information on capture and evolution of aerosols.

Capture process and interactions between the aerosols and nanofibres has been investigated.

Three types of aerosols were used:

- Wetting droplets (oil)
- Non-wetting droplets (water)
- Milled dust

Liu, C.; Hsu, P.-C.; Lee, H.-W.; Ye, M.; Zheng, G.; Liu, N.; Li, W.; Cui, Y. Nat. Commun. **2015**, 6, 6205

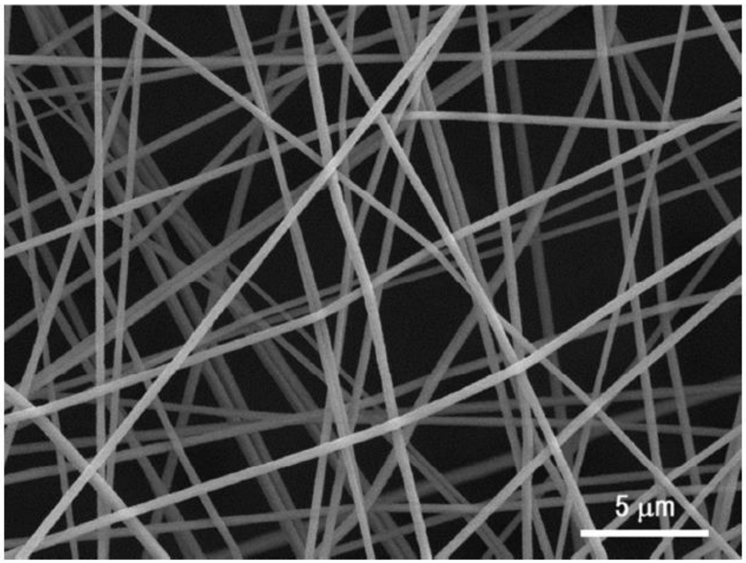

Fabrication of Polyimide Nanofibers by Electrospinning

The polyimide nanofibers were fabricated through electrospinning of polyimide N,N-dimethylformamide (DMF) solution. The solution system for the polymers used in this study was 15 wt % polyimide resin in DMF. A 1 mL syringe with a 22- gauge needle tip was used to load the polymer solution and connected to a voltage supply (ES30P-5W, Gamma High Voltage Research). A syringe pump (KD Scientific) was used to pump the solution out of the needle tip. The nanofibers were collected by a grounded copper mesh. The wire diameter of the copper mesh was 0.011 in., and the mesh size was 18 × 16. During electrospinning, the nanofibers would lie across the mesh hole to form the air filter.

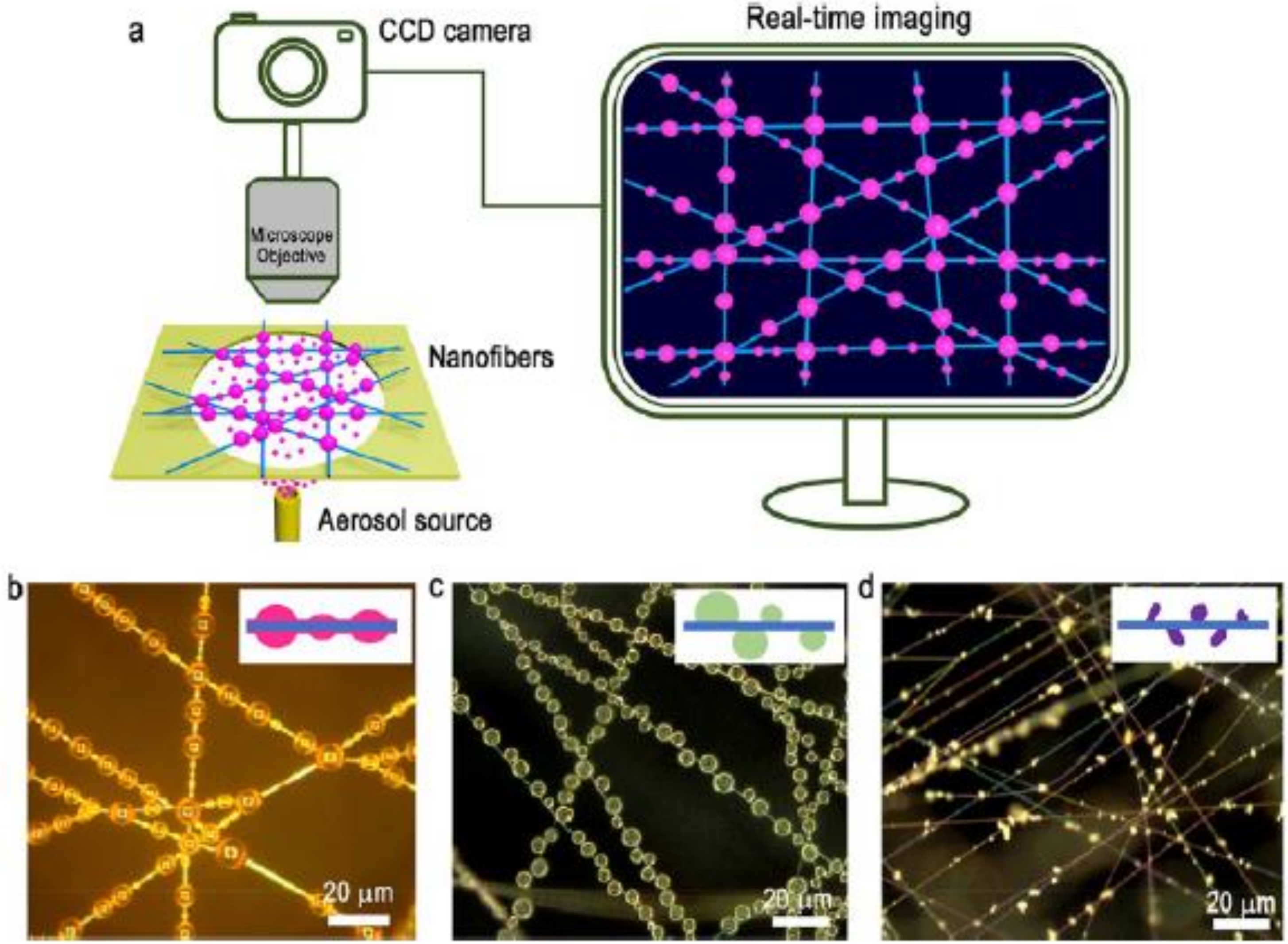

Schematic illustration of the in situ investigation on the nanoscale capture and evolution of aerosols on polyimide nanofibers and the typical images of different types of aerosols. (a) Illustration of the experimental setup. (b−d) Images of the in situ capture of (b) wetting droplets, (c) nonwetting droplets, and (d) solid particles by the nanofibers. Insets: Illustrations of the formation of wetting droplets, nonwetting droplets, and solid particles on the nanofibers.

Three distinct cases of conformation when a droplet with definite volume is placed on a cylindrical fiber with definite radius. (a) thin film; (b) axial-symmetric conformation connected with a thin film; (c) axial-asymmetrical conformation

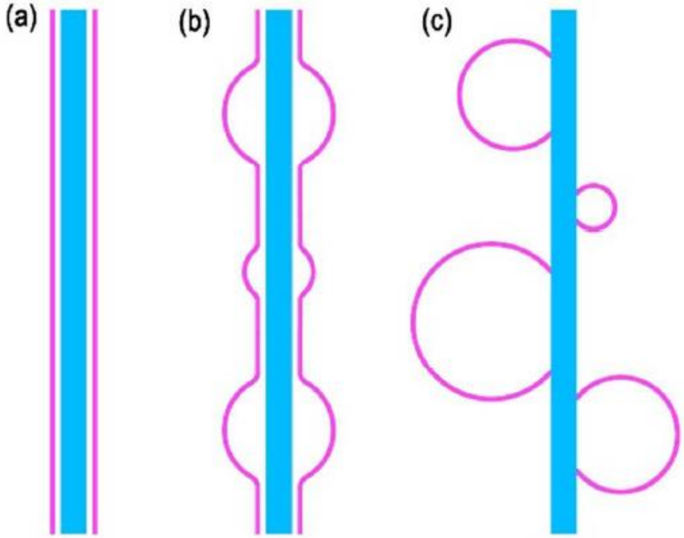

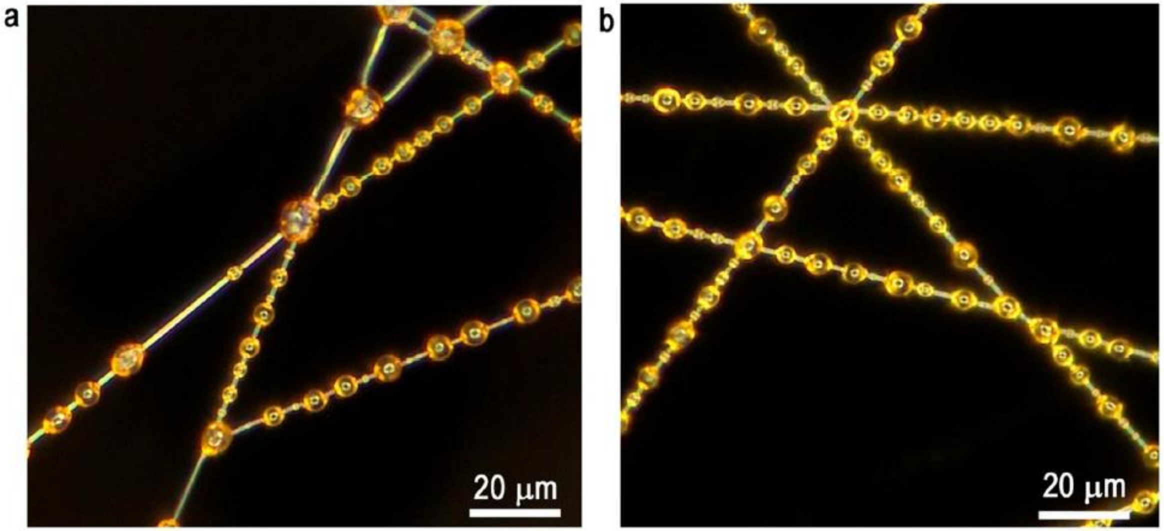

Optical images of solid particles evolved from oil droplets from (a) cigarette and (b) incense smoke captured on polyimide nanofibers after keeping in ambient conditions for two weeks.

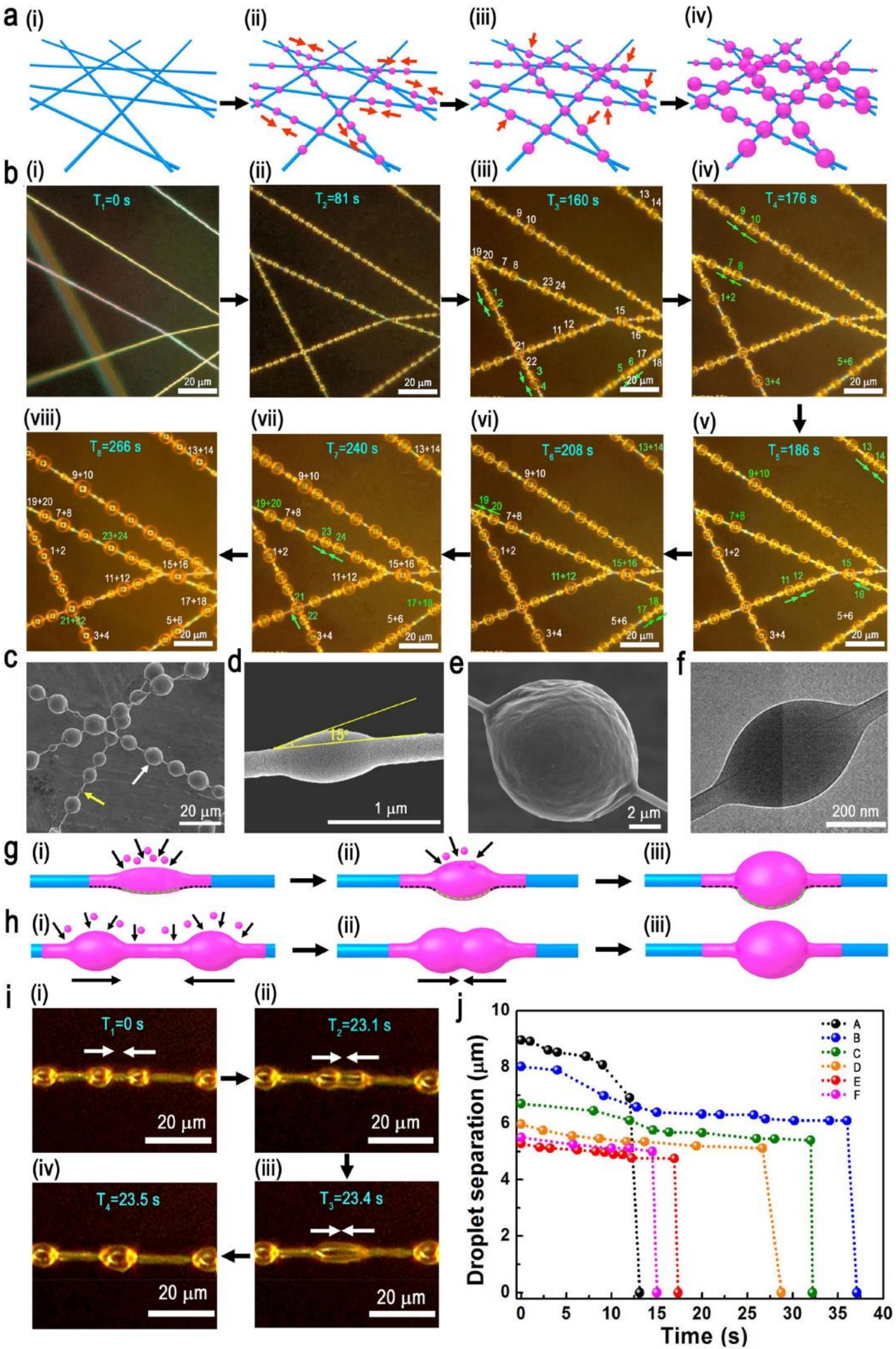

Capture, mobility, coalescence, and growth of oil droplets from cigarette smoke on polyimide nanofibers. (a) Schematic illustration of the capture, mobility, coalescence, and growth of oil droplets on polyimide nanofibers. a(i) A pristine polyimide nanofiber network. a(ii) The network begin to collect oil droplets with small diameters. a(iii) The adjacent captured droplets coalesce with each other. a(iv) The diameters of the droplets grow larger and larger. (b) Real-time imaging of the capture, mobility, coalescence, and growth of oil droplets on polyimide nanofibers. The numbers shown in these figures refer to the particles which will coalesce. (c−e) SEM and (f) TEM images of solid particles evolved by oil droplets from cigarette smoke after solidification. (g) Schematic illustration showing the process of new droplets merging into the pre-existing larger droplets on nanofibers. g(i) Small droplets begin to add onto a pre-existing droplet on the nanofiber. g(ii) and g(iii) The pre-existing droplet grow larger and larger with more small droplets being added in. The dashed black and green lines indicate the concave and convex sections of the outline of the longitudinal cross section of a droplet, respectively. (h) Schematic illustration of the coalescence process of adjacent oil droplets on nanofibers. h(i) Small droplets begin to add into two adjacent pre-existing droplets. h(ii) The two pre-existing droplets begin to connect with each other with more small droplets being added in. h(iii) The two-pre-existing droplets become a new larger one. i(i)−i(iv) The real-time images of the coalescence process of adjacent oil droplets on a nanofiber at different time. (j) The evolution of spatial separations of six pairs of droplets (labeled as A, B, C, D, E and F) on the nanofibers during the coalescence of adjacent droplets.

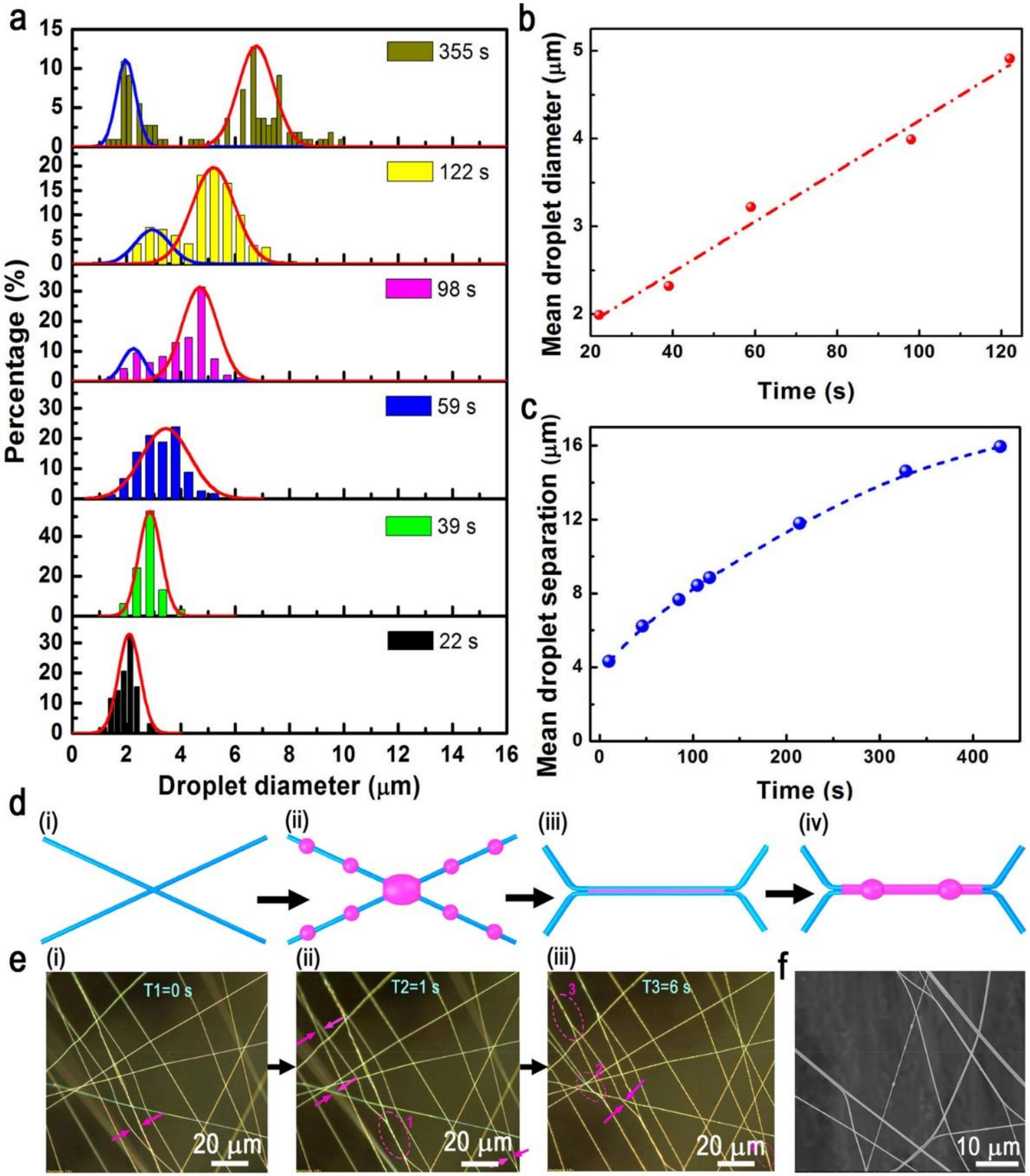

Diameter distribution of oil droplets from cigarette smoke on polyimide nanofibers and the adhesion of adjacent nanofibers. (a) The evolution of the diameter distribution of oil droplets. (b) The change of mean diameters of oil droplets over time. (c) The change of the mean droplet separations with time. (d) Schematic illustration of the adhesion of adjacent nanofibers caused by the capillary force of oil droplets between adjacent nanofibers. d(i) A pair of crossed nanofibers. d(ii) Some droplets are captured by the nanofibers. d(iii) The strong capillary force of oil droplets between two adjacent nanofibers causes the fibers to firmly adhere to each other. d(iv) With more droplets being captured by the two nanofibers, the coalesced nanofibers are completely coated by a layer of liquid and new droplets with larger diameters begin to appear on them. (e) Time-lapse images showing the adhesion of adjacent nanofibers by the oil droplets (indicated by four images labeled as i, ii, iii, and iv). The purple arrows and dashed ellipses indicate the nanofibers adhered together. (f) SEM image of adhered nanofibers.

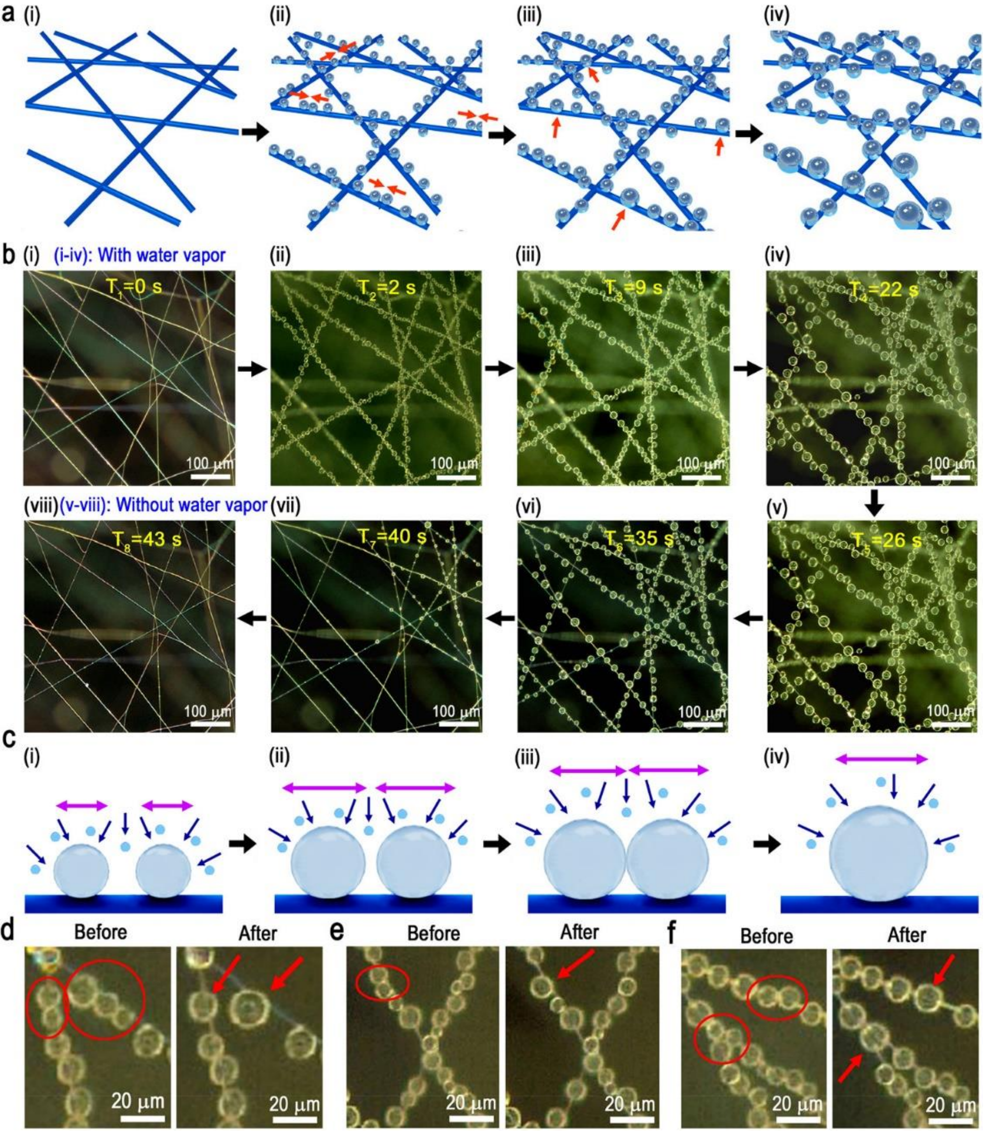

Capture of water droplets on polyimide nanofibers. (a) Schematic illustration of water droplet capture on polyimide nanofibers. a(i) A pristine polyimide nanofiber network. a(ii) The network begin capture water droplets with small diameters. a(iii) The captured small droplets begin to grow and coalesce with each other. a(iv) With more droplets being captured and coalesced with each other, the diameters of water droplets captured on this network become larger and larger. (b) Snapshots of real- time water droplet capture (i–iv) and evaporation (v–viii) process on polyimide nanofibers. From (i) to (iv), more and more small droplets are captured by the nanofibers and many of them coalesce with each other. From (v) to (viii), the diameters of water droplets become smaller and smaller and many of them disappear. (c) Schematic illustration of the coalescence of adjacent water droplets. c(i) Two adjacent water droplets. c(ii) With new small droplets being added, the two droplets begin to grow into larger ones. c(iii) With the increase of the diameter of the two droplets, their interspace becomes smaller and smaller. c(iv) Finally, the two droplets coalesce with each other. (d–f) Real-time images of the coalescence of adjacent water droplets.

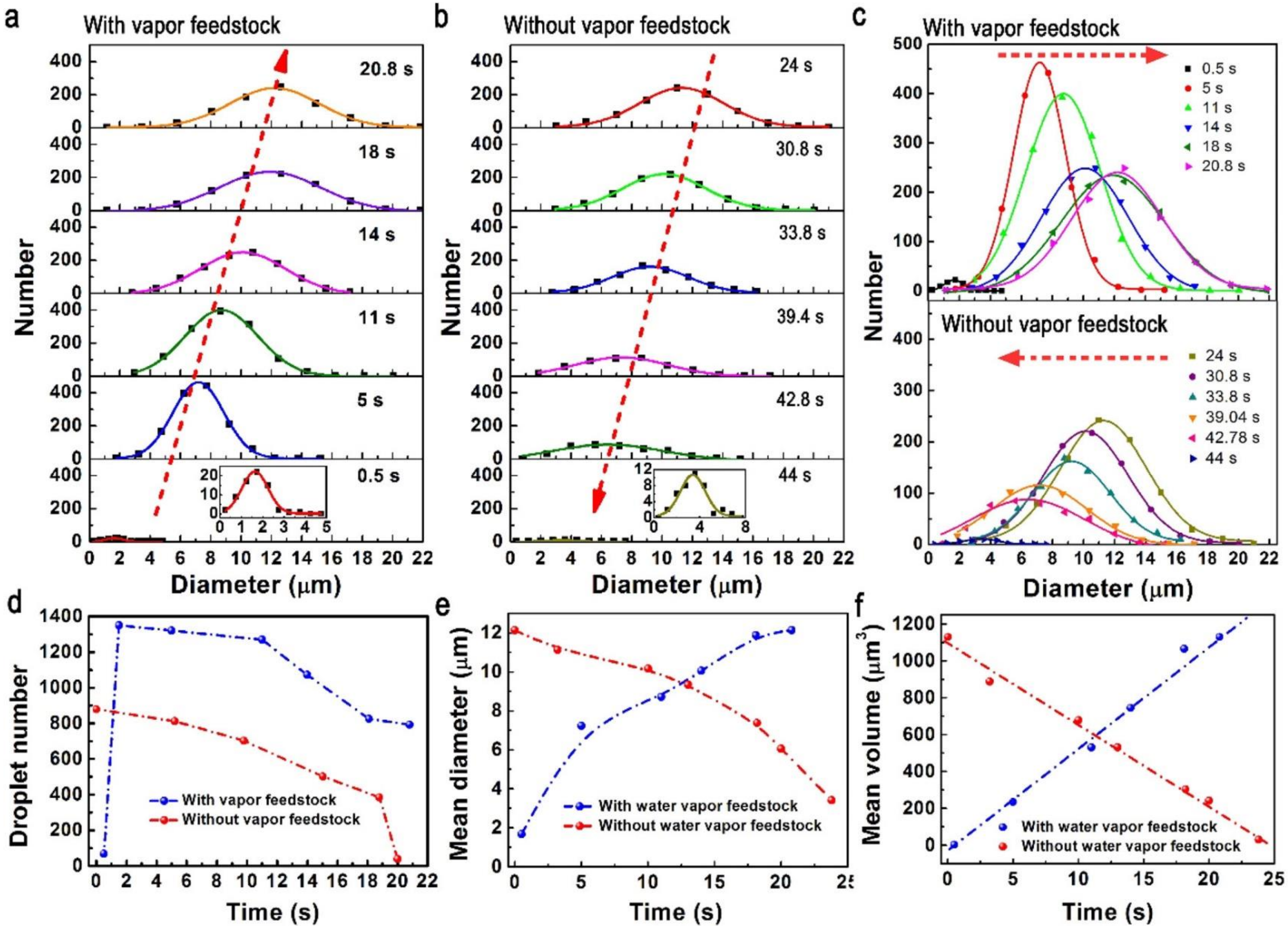

Diameter distribution of water droplets on polyimide nanofibers with and without water vapor feeding. (a) Number and diameter distribution variation during the capture of water droplets with water vapor feeding. (b) Number and diameter distribution variation during the evaporation of water droplets without water vapor feeding. (c) Comparison of number and diameter distribution of water droplets with and without water vapor feeding. (d–f) The variation of the droplet number (d), mean diameters (e), and mean volume (f) during the capture and evaporation of water droplets.

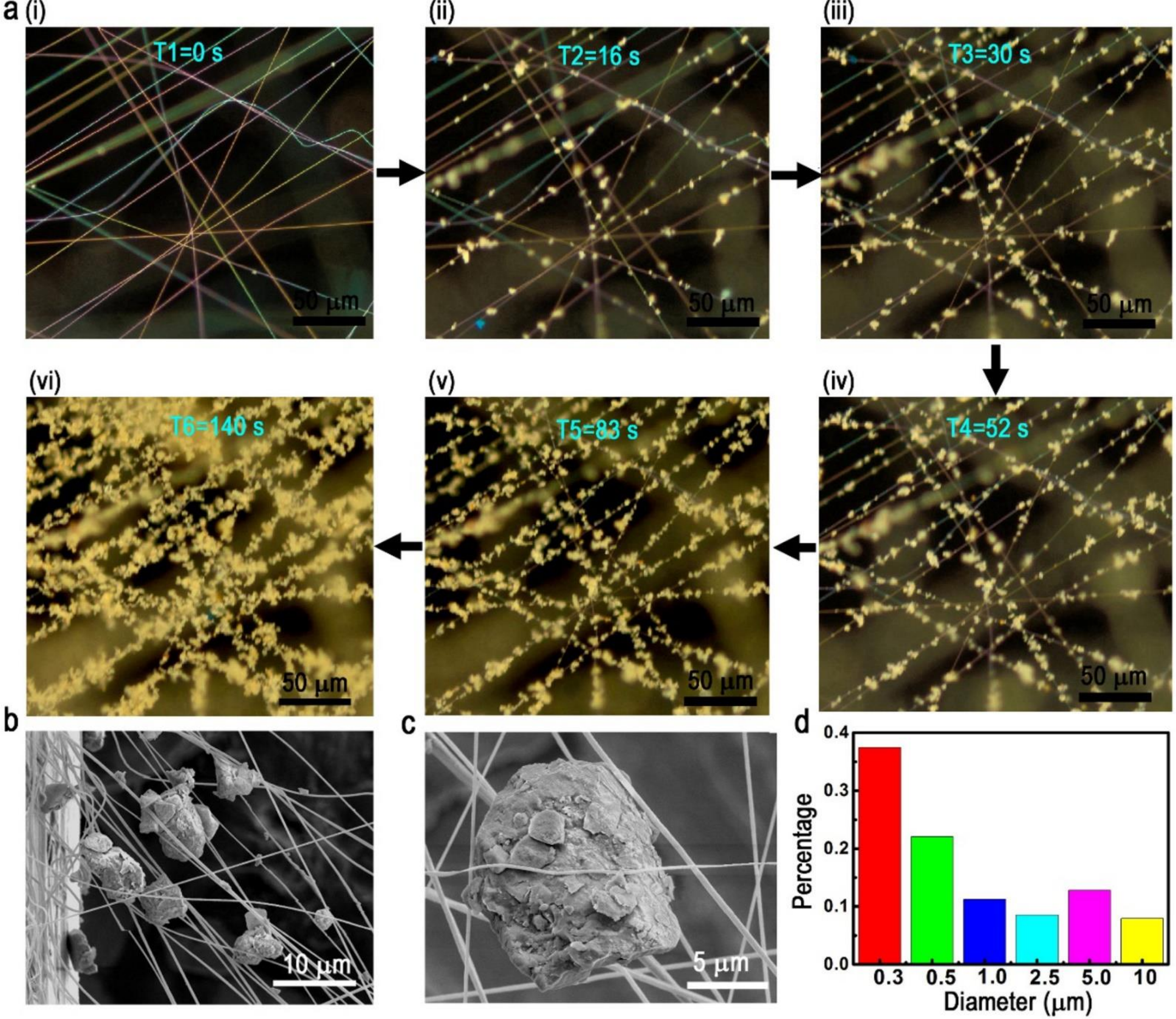

The capture, morphology, and size distribution of dust particles. (a) Snapshots of the real-time capture of dust particles on polyimide nanofibers. From (i) to (vi), more and more dust nanoparticles are captured by the nanofibers and they gradually form many dendrite-like structures. (b,c) SEM images of captured dust particles. (d) Size distribution of dust particles on nanofibers.

CONCLUSION

- For liquid droplet filtration and evolution, it depends on the surface tension. The wetting droplets had a small contact angle on polyimide nanofibers and formed axisymmetric conformations.
- The solids particles could neither completely wrap the nanofibers, nor more along them, but only attached to them with a small part of their weak van der Waals forces.
- For different type of aerosols require different structure design and surface modifications of fibres to tune the specific surface energy so as to enhance the wettability and adhesion to target aerosols on nanofibers.